A comparison of warm and combined warm and low temperature processing routes for the equal-channel angular pressing of pure titanium

Asli Günay Bulutsuz[*,1], Witold Chrominski[2], Yi Huang[3,4], Petr Kral[5], Mehmet Emin Yurci[1],
Malgorzata Lewandowska[2], Terence G. Langdon[4]

[1]Yildiz Technical University, Department of Mechanical Engineering, 34349 Besiktas, Istanbul, Turkey

[2]Warsaw University of Technology, Faculty of Materials Science and Engineering, Woloska 141, 02-507 Warsaw, Poland

[3]Department of Design and Engineering, Faculty of Science and Technology, Bournemouth University, Poole, Dorset BH12 5BB, U.K.

[4]Materials Research Group, Department of Mechanical Engineering, University of Southampton, Southampton SO17 1BJ, U.K.

[5]Institute of Physics of Materials, ASCR, Žižkova 22, CZ -61662 Brno, Czech Republic

Abstract

Two different processing routes were used to investigate the microstructure and strength of commercial purity (CP) titanium of grade 4 processed by equal-channel angular pressing (ECAP). In the combined temperature (CT) route the specimens were pressed at 723 K in the first pass and at 373 K in the second pass but in the warm temperature (WT) route the specimens were pressed through two passes at 723 K. Both routes led to an inhomogeneous microstructure with average grain sizes of ~1.5 and ~1.7 μm after the CT and WT routes, respectively. Both routes gave improved strengthening and higher hardness but the CT route with a lower temperature step gave the highest ultimate tensile strength of ~790 MPa. The inclusion of a lower temperature processing step may be important for optimizing the strength of CP Ti for use in medical implants.

This article has been accepted for publication and undergone full peer review but has not been through the copyediting, typesetting, pagination and proofreading process, which may lead to differences between this version and the Version of Record. Please cite this article as doi: 10.1002/adem.201900698

***Keywords*:** commercial purity titanium; equal-channel angular pressing; hardness; processing routes; ultrafine grains.

*Corresponding author: gunay@yildiz.edu.tr, +90 2123532959

1. Introduction

Experiments over the last three decades have established that the processing of metals using procedures based on the application of severe plastic deformation (SPD) provides an opportunity for achieving very significant grain refinement, typically to the submicrometer or even the nanometer range, combined with exceptional strengthening [1]. Processing by SPD refers specifically to the introduction of very high strains without incurring any significant changes in the overall dimensions of the work-pieces [2]. Although various SPD procedures are now available, the two primary processes are equal-channel angular pressing (ECAP) and high-pressure torsion (HPT) [3]. In practice, ECAP refers to the pressing of a bar or rod through a die constrained within a channel which is bent through an abrupt angle [4] whereas HPT denotes the torsional straining of a sample, usually in the form of a thin disk, during the application of a high applied pressure [5]. Both of these procedures produce excellent ultrafine-grained (UFG) microstructures but ECAP has an advantage because it entails the processing of larger samples which may provide opportunities for use in industrial applications. Furthermore, ECAP can be easily combined with other processes such as Conform for the production of relatively long rods of the UFG material [6, 7].

Commercial purity (CP) titanium is an excellent biomaterial but in practice it is generally strengthened with aluminum and vanadium to give the classic Ti-6Al-4V alloy which is used in many orthopedic and dental implants [8]. It is important to

recognize that this alloy was developed originally for use in aerospace applications and in practice there are long-term potential health problems associated with the release of Al and V ions into the human body so that these implants are generally restricted to service lifetimes of not more than 10-15 years [9]. One method for avoiding, or at least alleviating, the problem of inherent toxicity is to develop titanium alloys without the presence of any significant Al or V [10-13]. Yet another approach is to use SPD methods and other associated processing techniques in order to refine the grain size and thereby strengthen the commercial purity titanium without the addition of any alloying elements [14].

There are now several examples of this approach. For example, CP Ti of grade 4 was processed by ECAP and then subjected to thermo-mechanical processing in the form of forge stretching, drawing and annealing to give rods of 3 m length that were effectively cut for use as dental implants [15,16]. A CP Ti of grade 2 was subjected to ECAP and then cold rolled at a subzero temperature (173 K) to produce a tensile strength which slightly exceeded the traditional Ti-6Al-4V alloy [17]. Similarly, a CP Ti of grade 1 was successfully processed by ECAP at room temperature for 4 passes and then tested following the recommended standard for dental implants (International Organization of Standardization ISO 14801) to show that the fatigue life was significantly improved [18].

Accordingly, the present experiments were initiated in order to compare the potential for using a two-step processing route in which ECAP is used for two passes either at the same high temperature for both passes or with a significant drop in temperature for the second pass, where a major drop in temperature was selected to follow the earlier demonstration of the success of processing through the use of subzero rolling [17]. A CP Ti of grade 4 was selected for this investigation since this

represents the optimum pure material which may be used for medical implants based on considerations of toxicity.

2. Experimental material and procedures

The experimental material was commercial purity titanium (CP-Ti) of grade 4 which was annealed at 973 K for 4 h to give an initial average grain size of ~58 μm. According to the commercial specifications, the chemical composition of the material is given in Table 1.

Table 1 Composition of the commercially pure titanium grade 4

	N	C	O	Fe	H	Other,Total	Ti
Chemicals (wt%)	0.05%	0.08%	0.4%	0.5%	0.015%	0.4%	Balance

Billets for ECAP processing were cut as cylinders with lengths of 20 mm and diameters of 5 mm. These billets were processed using an ECAP die having an internal channel angle, Φ, of 110° and an outer arc of curvature, Ψ, close to 0°. These angles produce a strain of ~0.81 on each separate pass through the die [19]. After pressing for one pass, the billet was rotated about the longitudinal axis by 90° following the conventional processing route B_c [20]. Three sets of specimens were used in these experiments. First, and for comparison purposes, samples were examined directly without processing by ECAP. Second, billets were pressed for up to 2 passes using a ram speed of 0.1 mm/s following two different temperature

schemes: in the combined temperature (CT) scheme the specimens were initially pressed at 723 K in the first pass and then the second pass was conducted at 373 K whereas in the warm temperature (WT) scheme the specimens were pressed through two passes at 723 K. A lubricant containing MoS_2 was used for both sets of ECAP samples.

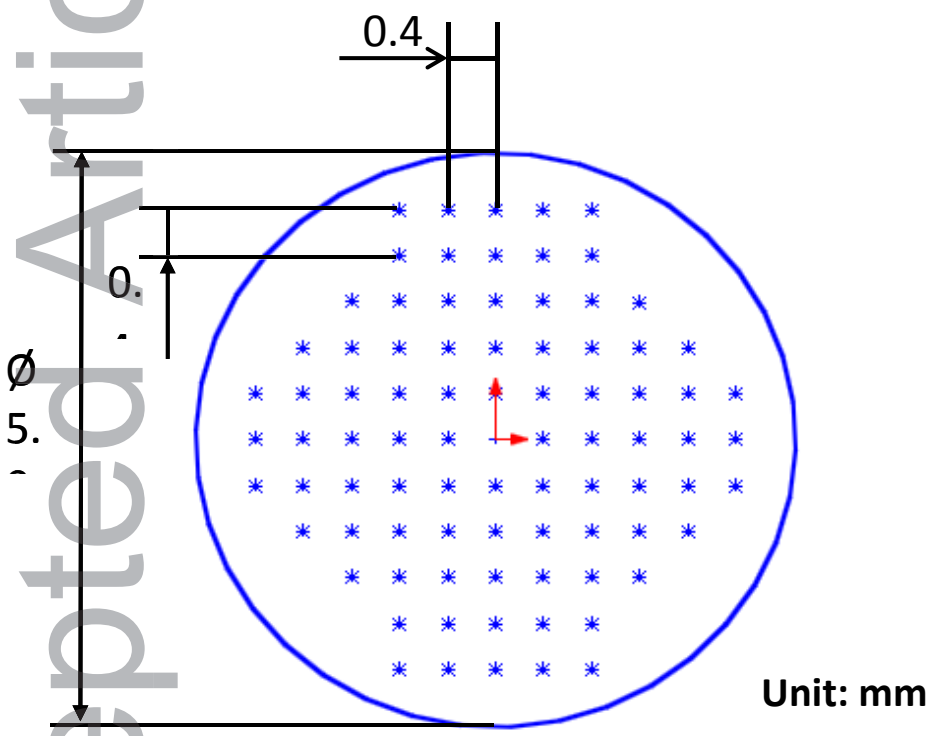

Figure 1 Schematic show of measurement points for hardness mapping.

The microstructures of all specimens were examined with an optical microscope and with a scanning electron microscope (SEM) on both polished and etched surfaces. The precipitate composition was examined at a 15 kV working voltage using an EDS spectra module of JED-2300, JCM 6000. For EBSD observations, a Tescan Lyra 3 SEM equipped with a NordlysNano EBSD detector was used with an accelerating voltage of 20 kV. The EBSD data were subsequently analyzed with HKL

Channel 5 software (Oxford Instruments). In order to determine the misorientations between grains, grain angles at and above 15° were designated high-angle grain boundaries (HAGBs) and angles between 2-15° were designated low-angle grain boundaries (LAGBs). For transmission electron microscopy (TEM), standard 3 mm disks were cut from the ECAP-processed billets and thin regions were prepared using double-jet polishing in a methanol-perchloric acid bath having a ratio of 4:1. The TEM observations were conducted in a JEOL JEM 1200 EX II microscope operating at 120 kV.

Dog-bone shape tensile specimens were cut from the central regions of the pressed billets with gauge lengths of 15.0 mm lying parallel to the pressing axes and with gauge widths and thicknesses of 4.0 and 1.5 mm, respectively. Specimens were cut by wire erosion and the surfaces were ground to remove any effects from the machining operation. A special tensile testing apparatus was fabricated to accommodate these small specimens in the tensile machine. Tensile tests were performed at room temperature under conditions of constant cross-head displacement using an initial strain rate of 1.0×10^{-3} s^{-1} and the stress-strain curves were then examined to determine the yield strength, σ_{ys}, the ultimate tensile strength, σ_{UTS}, and the elongation to failure, δ%.

A Vickers microhardness tester (HVS1000) was used to obtain hardness maps over the cross-sections of billets on surfaces cut perpendicular to the pressing direction. Measurements were taken at 85 different points on each surface using an array of 0.4 mm steps as depicted schematically in Figure 1 with each measurement taken using a load of 200 g for a dwell time of 10 s. These measurements were used to construct color-coded maps which provide visual displays of the microhardness values.

3. Experimental results

3.1 Microhardness measurements and tensile testing

The measured values of the mean microhardness for samples processed under these two processing conditions were Hv ≈ 272 for CT and Hv ≈ 245 for WT where, by multiplying by 9.807 N/mm^2, these values correspond to hardnesses of ~2670 and ~2400 MPa, respectively. By comparison, there was a measured microhardness of Hv ≈ 180 (~1770 MPa) for the initial annealed material without ECAP processing. Thus, processing by ECAP produces a significant increase in strength and hardness after only a single pass as noted also in earlier experiments conducted on a number of commercial aluminum-based alloys [21].

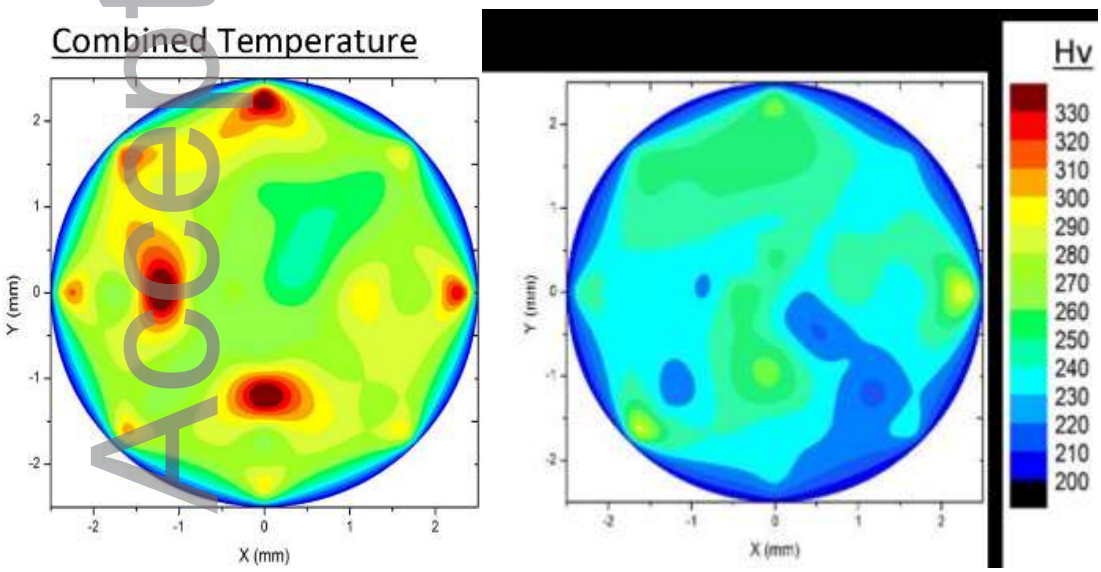

(a) (b)

Figure 2 Hardness mapping in ECAP processed samples under (a) CT and (b) WT conditions.

The homogeneity of the hardness measurements over the cross-sectional planes of the ECAP billets is shown by the color-coded maps presented in Figure 2 for processing under (a) CT and (b) WT conditions, respectively, where the data are plotted such that the *X* and *Y* scales are perpendicular orientations positioned arbitrarily such that the points (0,0) are located at the centers of the cross-sections of the two billets; the absolute values of the hardness values are indicated by the keys on the right of each diagram. Thus, the hardness is consistently higher for the CT scheme rather than the WT scheme and this is reasonable because of the potential for grain growth when pressing at higher temperatures. Nevertheless, there is a reasonable hardness homogeneity throughout the cross-sections for both processing conditions and there is no evidence for any regions of lower hardness, typically having thicknesses of ~0.5 mm, lying adjacent to the lower surfaces of the billets as reported earlier after processing of an Al-6061 alloy by up to 6 passes of ECAP at room temperature [22].

Table 2 Results from mechanical testing of specimens in the initial condition and after ECAP processing using the CT and WT processing routes.

Sample	Yield stress (MPa)	Ultimate tensile strength (MPa)	Ductility (δ/%)	Hardness (Hv)
Initial	550±13	610±15	32±0.2	180±5
CT	760±9	790±11	18±0.5	272±7
WT	710±6	760±7	22±0.3	245±3

In order to determine the strength of the specimens, tensile testing was conducted at room temperature using an initial strain rate of 1.0×10^{-3} s^{-1}. From these tests, the values of the yield stress (YS) and ultimate tensile strength (UTS) were recorded for the CT and WT conditions and the results are shown in Table 2 where the upper row corresponds to the initial annealed condition without ECAP processing. Thus, and consistent with the microhardness data, there is an increase in strength after ECAP processing and this increase is larger when processing following the CT scheme.

3.2 Microstructural evolution

Representative microstructures, obtained with optical microscopy and EBSD methods, are shown in Figures 3 and 4. The optical microscope images are given in Figure 3 for (a) the initial stare and (b) the CT and (c) WT states. As seen from the images in (a), (b) and (c), two passes of ECAP processing leads to a significant decrease in grain size. EBSD images are given in Figure 4 for samples processed under (a) CT and (b) WT conditions. Inspection of both images shows that there are inhomogeneous microstructures formed by a mixture of areas of ultrafine grains containing predominantly HAGBs and some exceptionally large grain areas containing predominantly LAGBs. Detailed inspection in EBSD suggests that Figure 4(a) contains a higher ratio of HAGBs than Figure 4(b). This is consistent with TEM observations where the microstructure in Figure 4(b) for the WT condition contained more subgrains and the ultrafine grain sizes tended to be relatively smaller than for the CT condition.

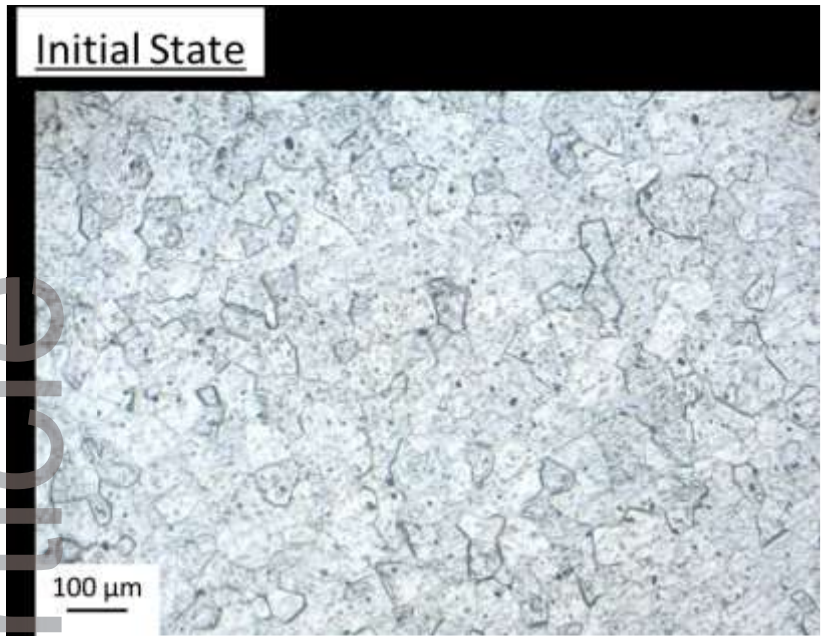

(a)

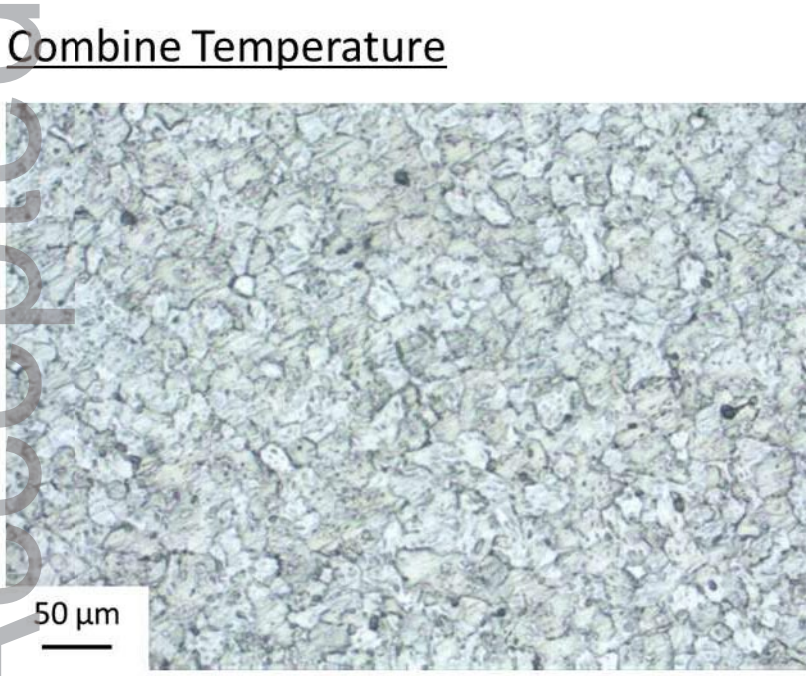

(b)

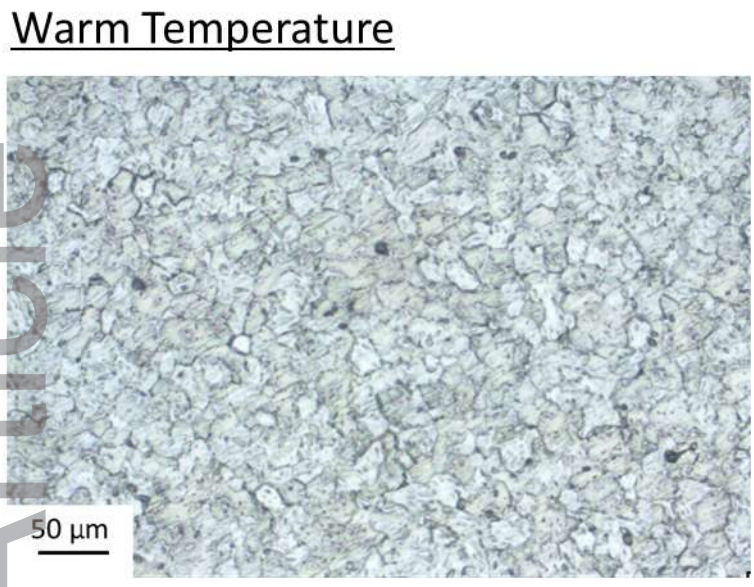

(c)

Figure 3 Optical microscope images of (a) initial state (b) CT and (c) WT conditions.

The grain size distributions are shown in Figure 5 for samples processed for 2 passes under (a) the CT and (b) the WT schemes. For the CT condition, the ultrafine grains occupy up to ~20 % of the total area and this is larger than for the WT condition. Nevertheless, several grains exceeding 10 µm were found in the CT microstructure and these large grains occupied ~30 % of the investigated area in this sample. The mean grain size in the CT sample was ~1.5 µm with no grains larger than ~17 µm whereas the mean grain size in the WT condition was ~1.7 µm with no grains larger than ~22.5 µm. Based on statistical analysis, the fraction of HAGBs in Figure 4(a) was estimated as ~45% and this is similar to, but slightly higher than, Figure 4(b) where it was ~40%.

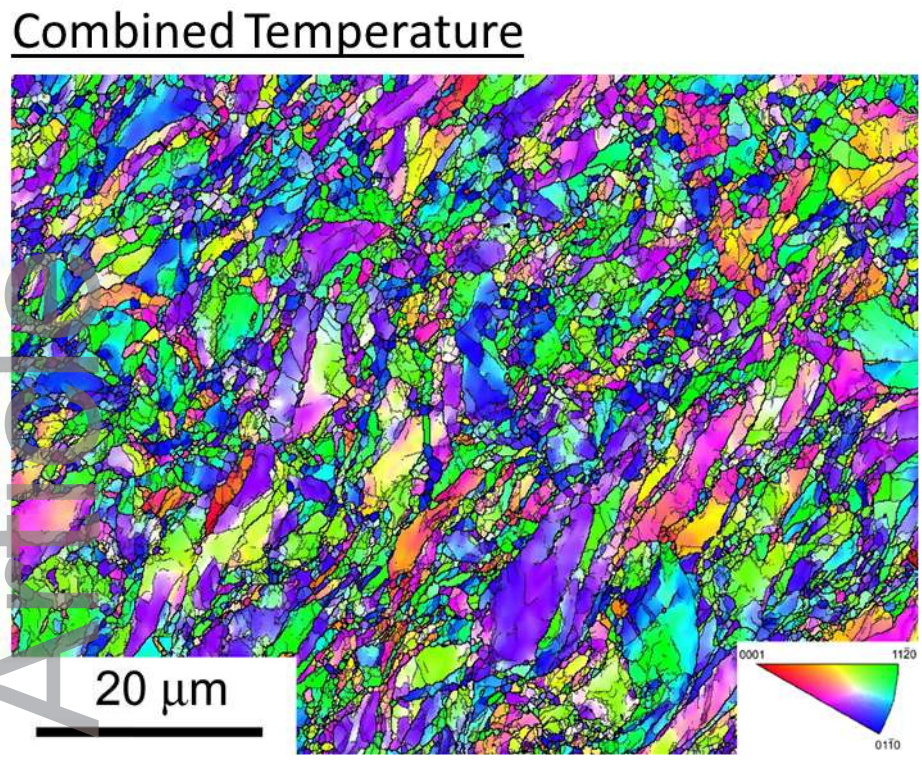

(a)

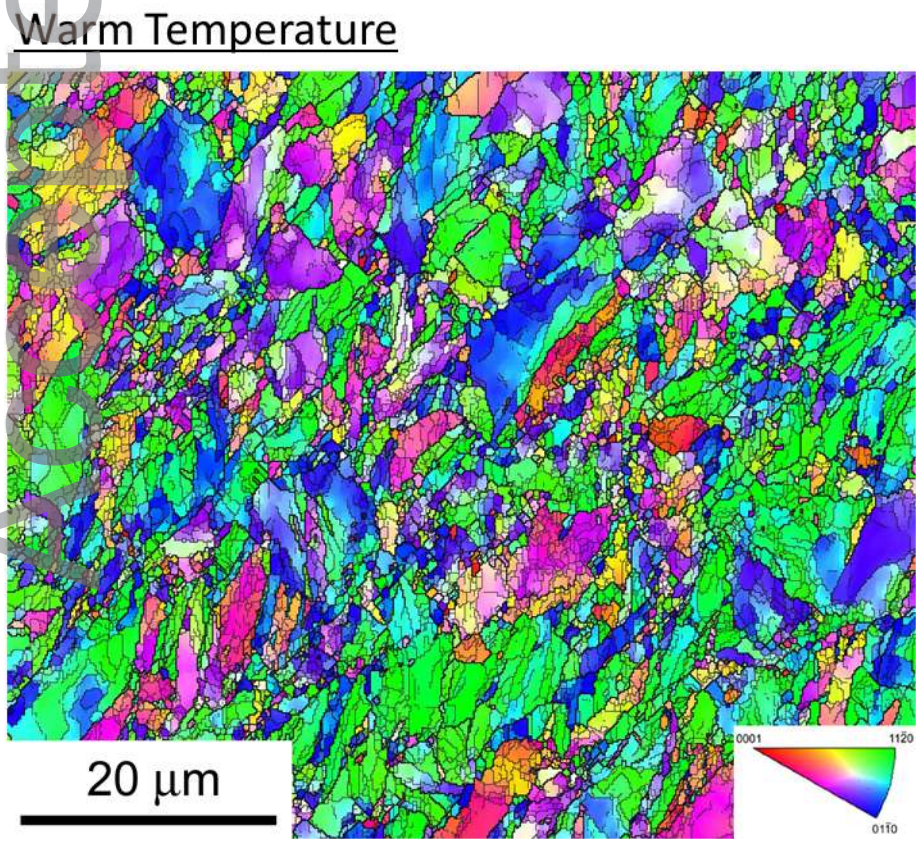

(b)

Figure 4 The EBSD orientation maps of samples processed by ECAP under (a) CT and (b) WT conditions.

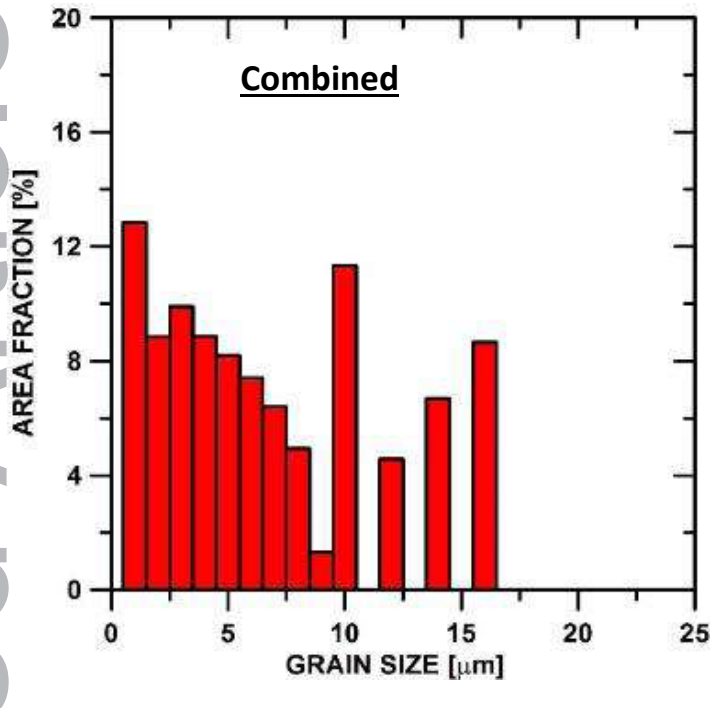

(a)

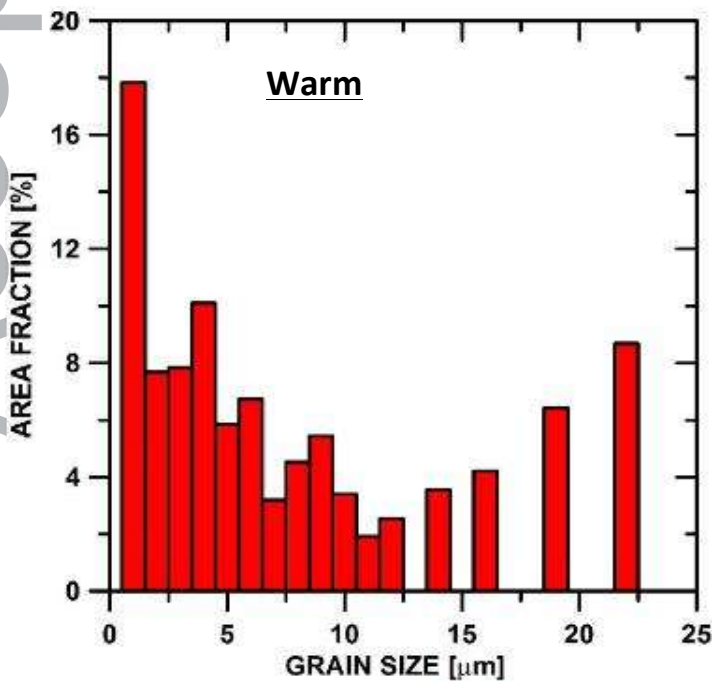

(b)

Figure 5 Grain size distribution in samples processed by ECAP under (a) CT and (b) WT conditions.

Figure 6 shows the inverse pole figures in (a) the CT sample and (b) the WT sample where (c) shows a schematic illustration of the ECAP die and (d) defines the coordinate system in the ECAP billet. In the CT sample in Figure 6(a), the basal poles of grains are tilted about 20-45° away from the *Y* axis and the many of the grains have a tendency to orient to $\{10\bar{1}2\}$ planes parallel with the pressing direction of the last pass where this corresponds to the longitudinal plane *XZ* parallel to the channel side wall. The $< 11\bar{2}0 >$ directions are oriented nearly parallel with the pressing direction which corresponds to the *X* axis. Thus, this microstructure for the CT sample has a relatively strong $\{10\bar{1}2\} < 11\bar{2}0 >$ microtexture. In the WT sample, Figure 6(b) shows the predominant tendency is to orient in the $< 11\bar{2}0 >$ directions parallel to the pressing direction and in the majority of grains there is a tendency to form basal poles parallel with the *Y* axis, where this means with {0001} planes parallel with the pressing direction of the last pass which corresponds again to the longitudinal plane *XZ* parallel to the channel side wall. Nevertheless, the texture of the WT sample appears more random than the CT sample and in the WT sample the microstructure has both relatively strong $\{0001\} < 11\bar{2}0 >$ and weak $\{10\bar{1}0\} < 11\bar{2}0 >$ microtextures.

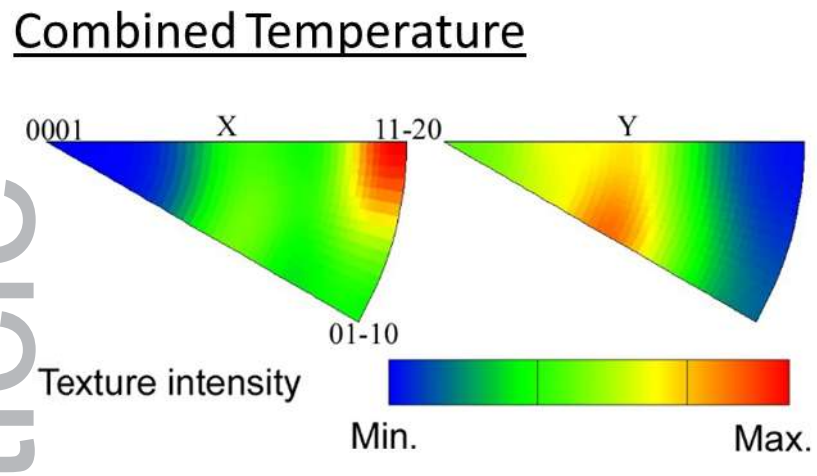

(a)

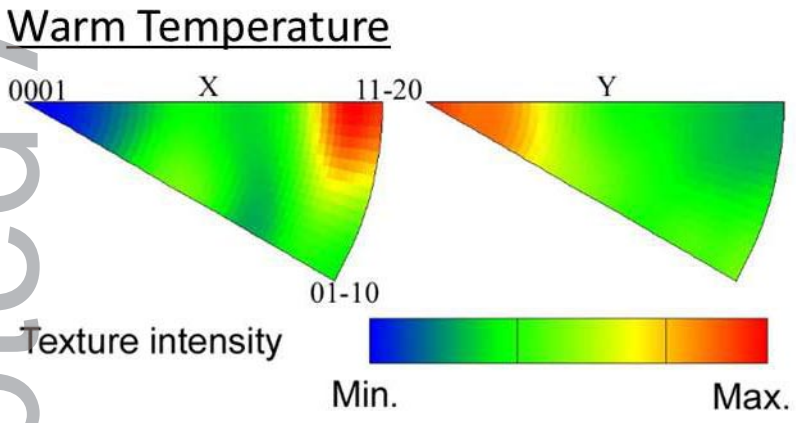

(b)

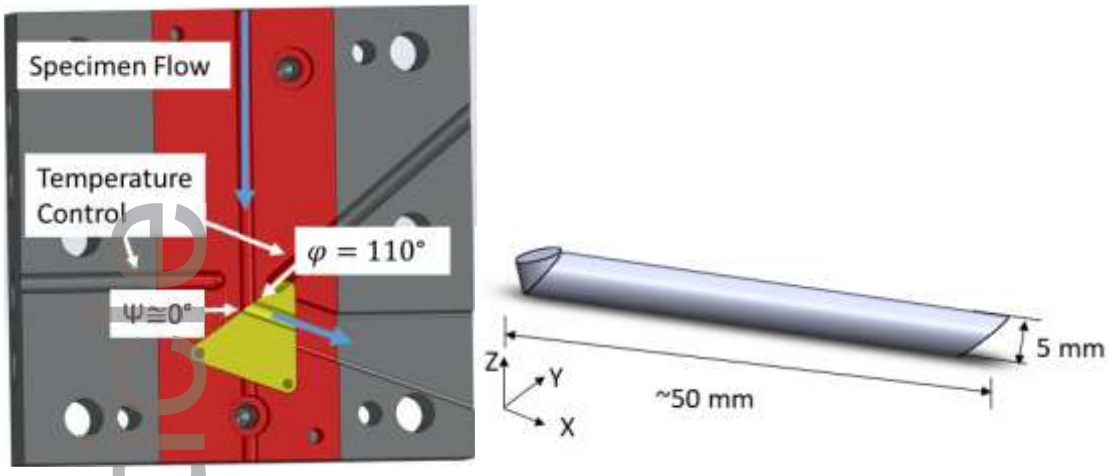

(c) (d)

Figure 6 Inverse pole figures obtained for the pressing direction (axis X) and longitudinal section (axis Y) in (a) CT sample; (b) WT sample; (c) ECAP die and (d) ECAP processing axis.

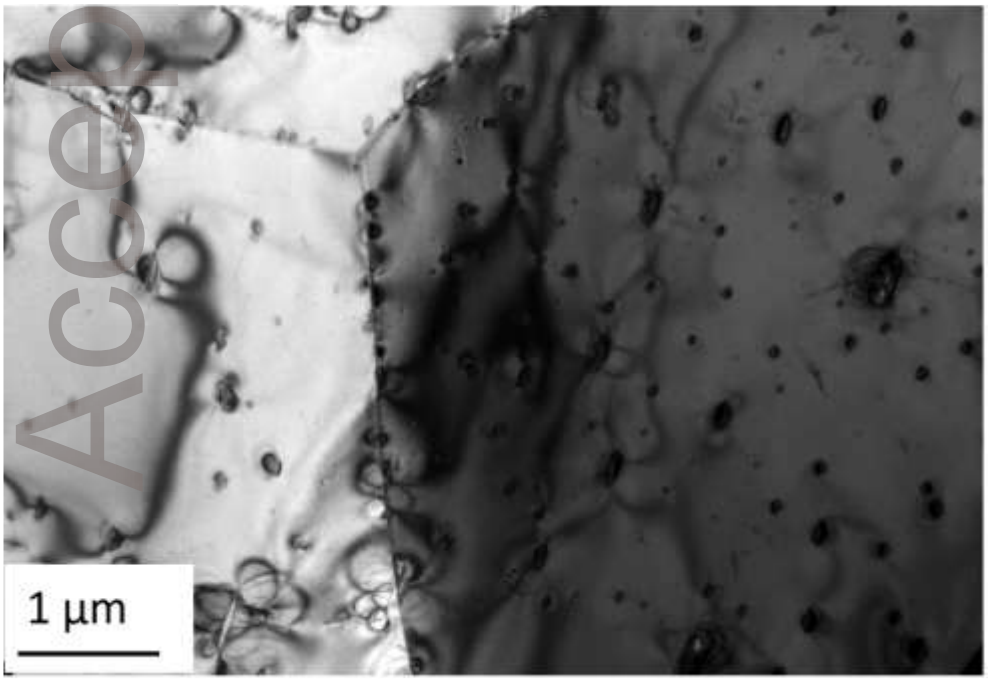

(a)

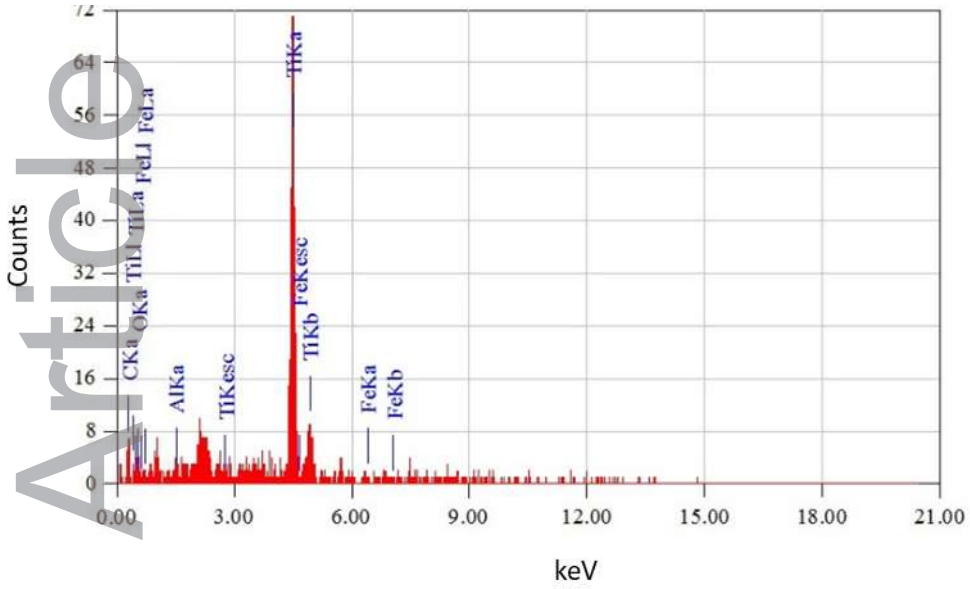

(b)

Figure 7 (a) TEM images of initial state of the sample and (b) SEM-EDS data showing precipitation.

In the initial unprocessed condition the average grain size was ~58 μm and there was evidence for some precipitate particles within the grains which can be seen in the TEM image of the initial state in Figure 7 (a). The precipitate composition was determined with SEM-EDS and the result is given in Figure 7 (b). Figure 8(a) shows a low magnification TEM image of material processed by ECAP under the CT scheme and a higher magnification image is shown in Figure 8(b). The non-uniform levels of shading in these images suggest the presence of high internal stresses which are a direct consequence of the SPD processing, where this is consistent with the detailed synchrotron X-ray microbeam diffraction measurements reported earlier for samples of an Al-1050 alloy processed by multiple passes of ECAP at room temperature [23].

Thus, there are almost no sharp changes in the strain contours which is a direct consequence of the residual stresses. From these observations, it is reasonable to conclude that there is only a single grain in the field of view in Figure 8(a). In the higher magnification image in Figure 8(b) there is a high density of dislocations within the observed area and these dislocations are relatively homogenously distributed. Again, the strain contours show non-uniform diffraction conditions in relatively small areas. It should be noted also that the dark contours are continuous so that there are no dislocation walls or LAGBs within this image.

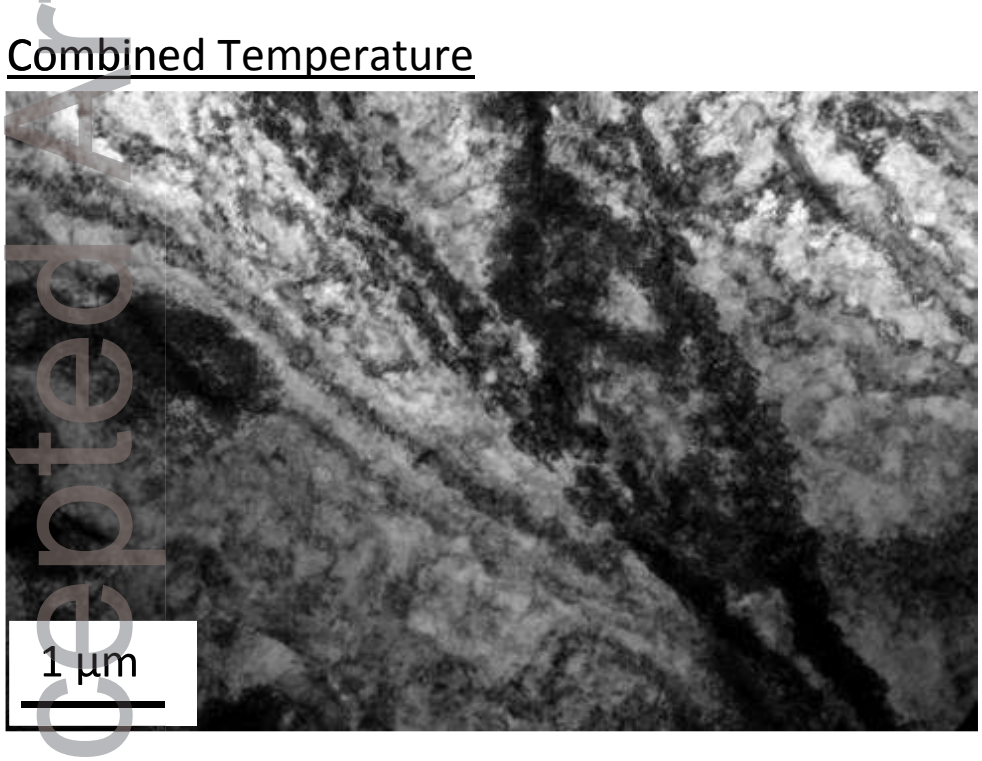

(a)

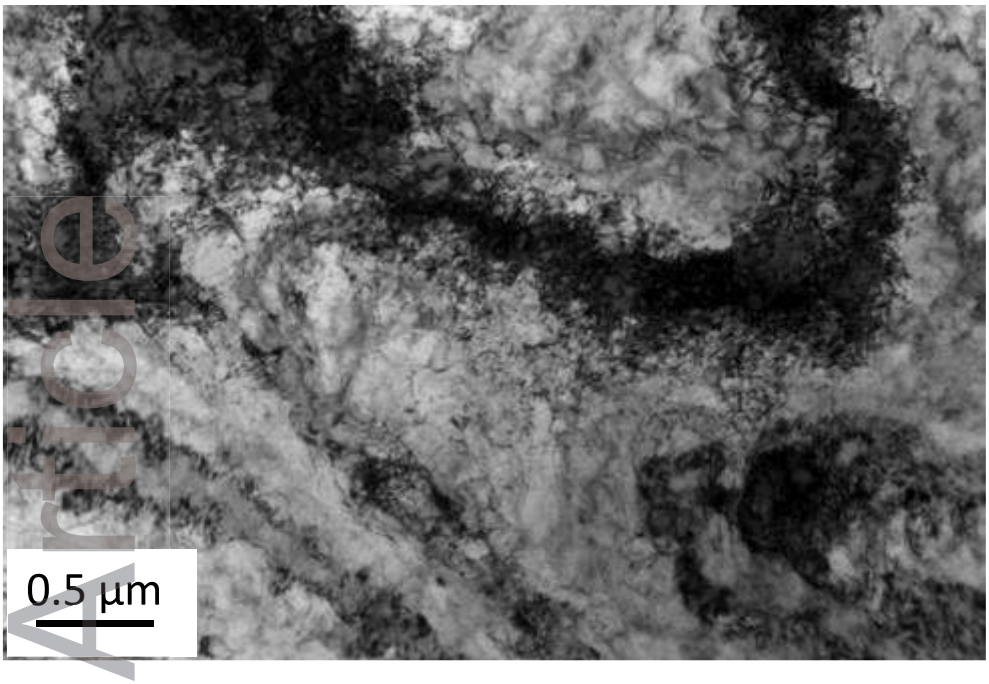

(b)

Figure 8 TEM images of CT sample with (a) lower and (b) higher magnifications

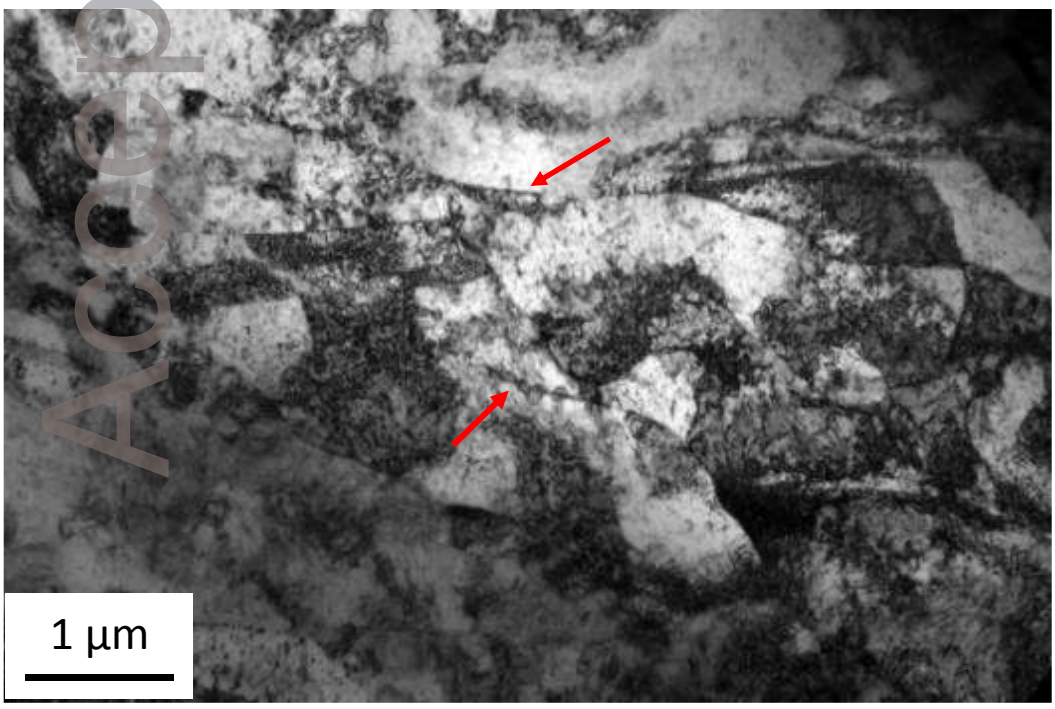

(a)

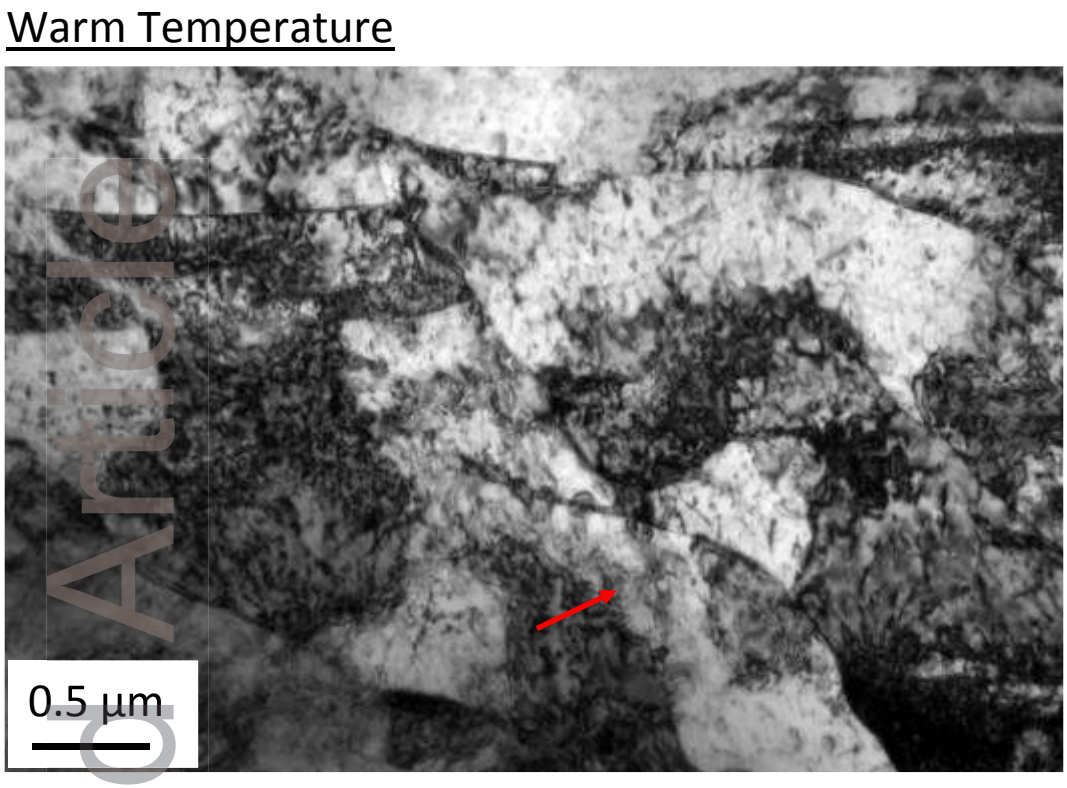

(b)

Figure 9 TEM images of WT sample with (a) lower and (b) higher magnifications

Similar sets of lower and higher magnification images are shown in Figure 9(a) and (b) for the WT conditions. In the lower magnification image in Figure 9(a) there are features that were not apparent in the CT images in Figure 8. Thus, the level of shading is again non-uniform over the whole image but there are sharp changes, marked with arrows, which denote the presence of LAGBs. In the higher magnification image in Figure 9(b) there are sub-grains filled with reasonably homogenously distributed dislocations and the neighboring grains vary in their contrast within the matrix which suggests slight differences in their individual orientations and/or in the local dislocation densities.

4. Discussion

These experiments examined two different processing routes for CP titanium of grade 4 where the CT route denotes an ECAP pass at 723 K followed by a pass at 373 K and the WT route denotes two consecutive passes at 723 K with all processing conducted using route B_C. In the unprocessed condition the Vickers microhardness was Hv ≈ 180 but after ECAP there was significant strengthening with values for Hv of ~272 and ~245 for the CT and WT routes, respectively. This increase in hardness was matched by an increase in the YS in tensile testing. For the unprocessed grade 4 material the measured YS was ~550 MPa which is close to the value of ~530 MPa reported earlier for CP Ti of grade 4 [24] but after processing the YS increased to ~760 and ~710 MPa for the CT and WT conditions, respectively. These values of the YS are generally high for CP Ti but they are lower than the reported values of ~915 MPa after 6 passes of ECAP and cold rolling [16], ~1006 MPa after 8 passes of ECAP and cold rolling [24] and ~1200 MPa after ECAP and a thermomechanical treatment involving forging and drawing [24].

All of these results are consistent and they demonstrate that some additional processing is required after ECAP in CP Ti in order to achieve the maximum YS. By contrast, high values of the YS may be achieved in appropriate Ti alloys after processing by ECAP without any additional processing: for example, a YS of ~1134 MPa was reported in a Ti-5.7Al-3.8Mo-1.2Zr-1.3Sn alloy after ECAP processing through 2 passes using a die with a channel angle of 120° at a temperature of 1023 K [26].

Examinations of the microstructures revealed inhomogeneity after both the CT and WT processing routes but this is reasonable since the processing was continued only

to 2 ECAP passes. Nevertheless, the average grain size was reduced from an initial value of ~58 μm to values of ~1.5 and ~1.7 μm after the CT and WT processing routes and there was a slightly higher fraction of ultrafine grains visible within the CT microstructure.

From early experiments on the processing of pure titanium by ECAP, it was concluded that the processing required a high pressing temperature of at least ~550 K [27] because, due to the limited number of active slip systems in titanium, processing at lower temperatures leads to a segmentation of the ECAP billets wherein the samples either break [27] or they became divided into discrete segments that are held together by small portions of material lying along the bottom surfaces of the billets [28]. In another study, experimental design was used to determine the optimal ECAP parameters for pure titanium of grade 4 and it was concluded that 573 K is the optimal processing temperature for a reasonably homogeneous microstructure [29].

Nevertheless, some other experiments demonstrated the feasibility of conducting the ECAP processing of CP-Ti of grade 1 at room temperature by using a low pressing speed, a higher channel angle of 120° or 135° and/or a special composite lubricant [30-33]. These experiments gave values for the YS of ~680 MPa after one pass [30] and after 8 passes it was ~710 MPa with a UTS of ~790 MPa [31]. A UTS of ~765 MPa was also reported after 4 passes at room temperature [33]. These latter values are very similar to the UTS values recorded in Table 2 after processing for 2 passes but the grain sizes were significantly smaller after the room temperature processing with values of ~0.20 μm [31] and ~0.15 μm [33], respectively. In practice, it is instructive to note that higher hardness values and even smaller grain sizes may be achieved when processing by HPT: for example, a grade 2 CP-Ti gave a grain

size of ~105 ± 12 nm and a hardness of Hv ≈ 320 ± 6 after processing by HPT for 20 turns at room temperature using an applied pressure of 6.0 GPa [34].

The various results obtained in the present experiments from tensile testing and hardness measurements, combined with the measured grain sizes, confirm that the CT processing route is preferable to the WT route for achieving optimum strength and mechanical properties. Therefore, it is reasonable to conclude that the introduction of a processing step at a lower temperature, either by conducting ECAP for at least one pass at a lower temperature as in the CT route or by subsequently introducing a new type of processing such as cold-rolling [17], may be advantageous in attaining the maximum strength when preparing CP Ti for use in aerospace applications or for medical implants.

5. Summary and conclusions

1. It is well known that CP is an excellent candidate material for use in biomedical implants but strengthening is required using a procedure such as ECAP.

2. CP Ti of grade 4 with an initial grain size of ~58 μm was processed using two different routes: a combined temperature (CT) route of an ECAP pass at 723 K and a second pass at 373 K and a warm temperature (WT) route of two ECAP passes at 723 K.

3. Both routes lead to improved strength, high hardness and an ultrafine microstructure but the CT route is preferable and the results demonstrate the need to include a lower temperature processing in order to optimize the strengthening effect.

4. The final grain sizes were ~1.5 and ~1.7 μm after the CT and WT routes, respectively, but both microstructures exhibited significant inhomogeneity.

Acknowledgements

The authors thank the Technical Electrical Materials Industry and Trade Inc. for their technical support. Two of the authors (YH and TGL) were supported by the European Research Council under ERC Grant Agreement no. 267464-SPDMETALS. The microstructural part of this research was supported by the statutory funding of the Faculty of Materials Science and Engineering of Warsaw University of Technology.

References

[1] R.Z. Valiev, R.K. Islamgaliev, I. V. Alexandrov, *Prog. Mater. Sci.* **2000**, *45*, 103..

[2] R.Z. Valiev, Y. Estrin, Z. Horita, T.G. Langdon, M.J. Zehetbauer, Y. Zhu, *JOM* **2016**, *68*, 1216.

[3] T.G. Langdon, *Acta Mater.* **2013**, *61*, 7035.

[4] R.Z. Valiev, T.G. Langdon, *Prog. Mater. Sci.* **2006**, *51*, 881.

[5] A.P. Zhilyaev, T.G. Langdon, *Prog. Mater. Sci.* **2008**, *53*, 893.

[6] G.J. Raab, R.Z. Valiev, T.C. Lowe, Y.T. Zhu, *Mater. Sci. Eng. A* **2004**, *382*, 30.

[7] C. Xu, S. Schroeder, P.B. Berbon, T.G. Langdon, *Acta Mater.* **2010**, *58*, 1379.

[8] C.N. Elias, J.H.C. Lima, R. Valiev, M. a Meyers, *JOM.***2008**, *60(3)*, 46.

[9] M. Geetha, A.K. Singh, R. Asokamani, A.K. Gogia, *Prog. Mater. Sci.* **2009**, *54*, 397.

[10] Y. Okazaki, Y. Ito, A. Ito, T. Tateishi, *Mater. Trans. JIM* **1993**, *34*, 1217.

[11] Y. Okazaki, Y. Ito, K. Kyo, T. Tateishi, *Mater. Sci. Eng. A* **1996**, *213*, 138.

[12] Y. Okazaki, S. Rao, T. Tateishi, Y. Ito, *Mater. Sci. Eng. A* **1998**, *243*, 250.

[13] Y. Okazaki, S. Rao, Y. Ito, T. Tateishi, *Biomaterials* **1998**, *19*, 1197.

[14] Y. Estrin, R. Lapovok, A.E. Medvedev, C. Kasper, E. Ivanova, T.C. Lowe, *Titanium in Medical and Dental Applications*.**2018**, pp.419-454, Woodhead Publishing in Biomaterials, Elsevier.

[15] R.Z. Valiev, I.P. Semenova, E. Jakushina, V.V. Latysh, H.J. Rack, T.C. Lowe, J. Petruželka, L. Dluhoš, D. Hrušák, J. Sochová, *Mater. Sci. Forum* **2008**, *584–586*, 49.

[16] L.R. Saitova, H.W. Höppel, M. Göken, I.P. Semenova, G.I. Raab, R.Z. Valiev, *Mater. Sci. Eng. A* **2009**, *503*, 145.

[17] V.L. Sordi, M. Ferrante, M. Kawasaki, T.G. Langdon, *J. Mater. Sci.* **2012**, *47*, 7870.

[18] R.B. Figueiredo, E.R.de C. Barbosa, X. Zhao, X. Yang, X. Liu, P.R. Cetlin, T.G. Langdon, *Mater. Sci. Eng. A* **2014**, *619*, 312.

[19] Y. Iwahashi, J. Wang, Z. Horita, M. Nemoto, T.G. Langdon, *Scr. Mater.* **1996,** *35,* 143.

[20] M. Furukawa, Y. Iwahashi, Z. Horita, M. Nemoto, T.G. Langdon, *Mater. Sci. Eng. A* **1998,** *257,* 328.

[21] Z. Horita, T. Fujinami, M. Nemoto, T.G. Langdon, *Metall. Mater. Trans. A* **2000**, *31*, 691.

[22] M. Prell, C. Xu, T.G. Langdon, *Mater. Sci. Eng. A* **2008**, *480*, 449.

[23] T.Q. Phan, L.E. Levine, I.F. Lee, R. Xu, J.Z. Tischler, Y. Huang, T.G. Langdon, M.E. Kassner, *Acta Mater.* **2016**, *112*, 231.

[24] R.Z. Valiev, I.P. Semenova, V. V. Latysh, H. Rack, T.C. Lowe, J. Petruzelka, L. Dluhos, D. Hrusak, J. Sochova, *Adv. Eng. Mater.* **2008**, *10*, 15.

[25] A. Chakraborty, P.K. Chakraborty, P. Banik, D.K. Bagchi, *Indian J. Agron.* **2001**, *46*, 75.

[26] I.P. Semenova, G.S. Dyakonov, G.I. Raab, Y.F. Grishina, Y. Huang, T.G. Langdon, *Adv. Eng. Mater.* **2018**, *20*, 1.

[27] S.L. Semiatin, D.P. DeLo, V.M. Segal, R.E. Goforth, N.D. Frey, *Metall. Mater. Trans. A* **1999**, *30*, 1425.

[28] P.R. Cetlin, M.T.P. Aguilar, R.B. Figueiredo, T.G. Langdon, *J. Mater. Sci.* **2010**, *45*, 4561.

[29] A.G. Bulutsuz, M.E. Yurci, N. Durakbaşa, Mater. Res. 2018, 21, doi: 10.1590/1980-5373-mr-2018-0270

[30] X. Zhao, W. Fu, X. Yang, T.G. Langdon, *Scr. Mater.* **2008**, *59*, 542.

[31] X. Zhao, X. Yang, X. Liu, X. Wang, T.G. Langdon, *Mater. Sci. Eng. A* **2010**, *527*, 6335.

[32] Y. Zhang, R.B. Figueiredo, S.N. Alhajeri, J. Tao, N. Gao, T.G. Langdon, *Mater. Sci. Eng. A* **2011**, *528*, 7708.

[33] X. Zhao, X. Yang, X. Liu, C.T. Wang, Y. Huang, T.G. Langdon, *Mater. Sci. Eng. A* **2014**, *607*, 482.

[34] C.T. Wang, A.G. Fox, T.G. Langdon, *J. Mater. Sci.* **2014**, *49*, 6558.

The effect of combined low (373 K) and warm temperature (723 K) route effect on microstructure and mechanical properties are determined for CP Ti. After two passes the samples have an inhomogeneous microstructure and hardness distribution. For the lower temperature route, the specimen has the highest strength. The inclusion of a lower temperature processing step is important for optimizing the strength of CP Ti.